Title

Cooperativity between Al Sites Promotes Hydrogen Transfer and Carbon–Carbon Bond Formation upon Dimethyl Ether Activation on Alumina

Journal

ACS Central Science, 1(6)

ISSN

2374-7943

Authors

Comas-Vives, Aleix
Valla, Maxence
Copéret, Christophe
et al.

Publication Date

2015-09-23

DOI

10.1021/acscentsci.5b00226

Peer reviewed

ACS central science

Research Article

http://pubs.acs.org/journal/acscii

Cooperativity between Al Sites Promotes Hydrogen Transfer and Carbon−Carbon Bond Formation upon Dimethyl Ether Activation on Alumina

Aleix Comas-Vives,[†,#] Maxence Valla,[†,#] Christophe Copéret,[*,†] and Philippe Sautet[*,‡]

[†]Department of Chemistry and Applied Biosciences, ETH Zürich, Vladimir Prelog Weg 1-5, CH-8093 Zürich, Switzerland

[‡]CNRS, Institut de Chimie de Lyon, École Normale Supérieure de Lyon, Université de Lyon, 46 allée d'Italie, F-69364 Lyon Cedex 07, France

Supporting Information

ABSTRACT: The methanol-to-olefin (MTO) process allows the conversion of methanol/dimethyl ether into olefins on acidic zeolites via the so-called hydrocarbon pool mechanism. However, the site and mechanism of formation of the first carbon−carbon bond are still a matter of debate. Here, we show that the Lewis acidic Al sites on the 110 facet of γ-Al_2O_3 can readily activate dimethyl ether to yield CH_4, alkenes, and surface formate species according to spectroscopic studies combined with a computational approach. The carbon−carbon forming step as well as the formation of methane and surface formate involves a transient oxonium ion intermediate, generated by a hydrogen transfer between surface methoxy species and coordinated methanol on adjacent Al sites. These results indicate that extra framework Al centers in acidic zeolites, which are associated with alumina, can play a key role in the formation of the first carbon−carbon bond, the initiation step of the industrial MTO process.

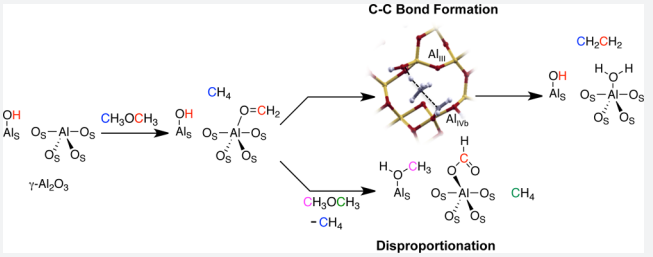

Forming carbon−carbon bonds from C_1 species is a long-standing scientific and industrial challenge.[1−15] An industrial breakthrough stemmed from the discovery of the methanol to olefin (MTO) process in the 1970s, which allowed the catalytic conversion of methanol to ethylene and propylene by zeolites (Scheme 1). This process constitutes an alternative route to light

Scheme 1. Methanol to Olefin Process Catalyzed by Zeolites

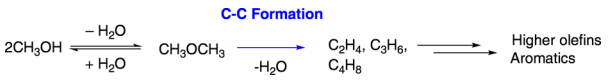

alkenes not relying on crude oil. Several industrial plants are being opened, in particular in Asia, in view of the increasing demand for alkene feedstocks.[16,17]

The mechanism of this process is a matter of intense debate and investigation both in industry and academia.[17−31] Initially, direct pathways from methanol to olefin were suggested (Scheme 2b−e), but in the 1990s Dahl and Kolboe proposed an indirect pathway that proceeds via a hydrocarbon pool as shown in Scheme 2a.[32−34] A dual operating cycle,[30,31] one for alkenes (Scheme 2a, left) and another one for aromatics (Scheme 2a, right), forms the currently accepted mechanism operating under industrial MTO conditions. Carbenium species have been proposed as the active species of the hydrocarbon pool cycle,[18] and a complete catalytic cycle combining theory and experiment was proposed for the HZSM-5 zeolite.[20,35]

Nevertheless, the question related to the site and mechanism of formation of the first olefins and aromatics, requiring carbon−carbon bond forming processes from methanol/dimethyl ether, has remained a matter of debate. More than 20 mechanisms have been proposed for this step,[17,28] involving intermediates such as methane−formaldehyde,[23] oxonium ylide,[27] and carbenoid or alkoxy species (Scheme 2b−e), and some proposals also include the presence of adventitious organic compounds such as aromatics. Extensive attention was devoted to the oxonium ylide mechanism (Scheme 2c), which by an intramolecular Steven's rearrangement would produce methylethyl ether, which could then form ethene by β-hydride elimination. This mechanism and parent ones were discarded because of the need for formation of highly unstable oxonium ylide species.[22,36] Other direct C−C bond formation routes, via methane-formaldehyde (Scheme 2b) or carbenoid species (Scheme 2d), were found unfavorable on the basis of an extensive *ab initio* study.[25] It is worth noting that all the zeolites active in the MTO process contain Al sites. This element provides acidic sites that play a significant role in the zeolite catalytic activity, and they could participate in the initial carbon−carbon bond formation step. Moreover, there is always a debate whether or not extraframework aluminum, which is in the form of alumina, could be responsible for side-reactions in zeolite catalysis.[37−39] Hence,

Received: June 6, 2015
Published: August 5, 2015

DOI: 10.1021/acscentsci.5b00226
ACS Cent. Sci. 2015, 1, 313−319

Scheme 2. A Selection out of the More than 20 Proposed Mechanisms for the Carbon−Carbon Bond Formation Step Is Shown: (a) Hydrocarbon Pool, (b) Methane-formaldehyde Route, (c) Oxonium-ylide, (d) Carbine-carbenoid Mechanisms, (e) Alkoxy Mechanism

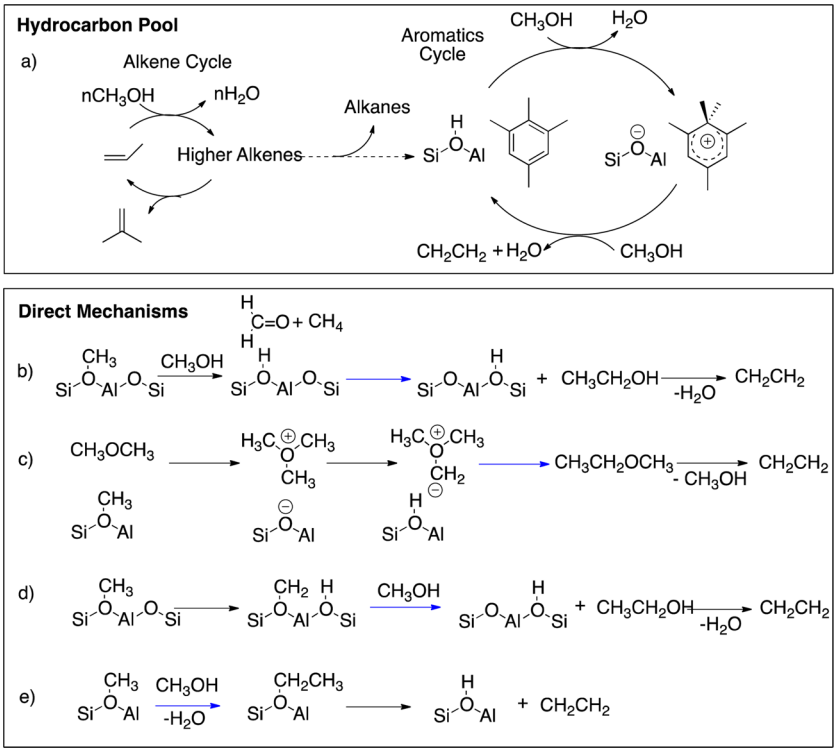

one important aspect that has not been considered is the participation of multiple Al centers, possibly belonging to alumina, in the promotion of carbon−carbon bonds in the MTO process. Though the formation of hydrocarbons by reaction of methanol on alumina or silica−alumina was reported,[40] most studies have concentrated on the hydrolysis of dimethyl ether (DME) into methanol and the reverse reaction and also on the alcohol dehydration to the corresponding ether and olefins.[41−54] Recent works have shown that γ-Al_2O_3 and δ-Al_2O_3 contain on their 110 facet[55] highly reactive tricoordinated Al_{III} and four-coordinated Al_{IVb} sites, which are able to activate the C−H bond of methane at low temperatures (<150 °C)[56,57] and to convert CH_3F into branched olefinic products isobutene and 2-methylbutene at relatively mild temperatures (200 °C) showing that the key carbon−carbon formation step occurs on alumina surfaces via the growth of surface alkoxy chains.[58] In such processes, adsorbed water plays a key role to facilitate the activation of hydrocarbons, through the formation of basic O sites and the stabilization of the otherwise unstable 110 facet.[57,59]

Here, we show that alumina converts DME at 300 °C into methane along with smaller amounts of higher olefin products, such as ethene, propene, butenes, and pentenes, analogously to the MTO process. In addition, combined IR and solid-state NMR show that this process is accompanied by the formation of methoxy and formate surface species besides methane and other hydrocarbons detected in the gas phase. *Ab initio* simulations suggest a step involving a hydride transfer from a methoxy aluminum surface species and an activated DME, adsorbed on adjacent Al sites. This process involves a transition state structure with an oxonium ($AlO{=}CH_2^+$)/methane adduct, which evolves either to the formation of methane and adsorbed formate species or olefins through a carbon−carbon bond forming process, consistent with experimental observation. This indicates that two Al sites can play in concert to generate $AlO{=}CH_2^+$ species as key transient species, able to activate C−H bonds and to promote a C−C bond formation step.

First, the reaction of DME (0.05 mmol) with alumina (Evonik aluC, 130 $m^2 \cdot g^{-1}$ or SBA, 200 $m^2 \cdot g^{-1}$) partially dehydroxylated at 700 °C was monitored by gas chromatography as a function of temperature (Table 1a and Table S1). Methane evolved at 300 °C,[60] 0.029 mmol as a sole gaseous product, which corresponds

Table 1. (a) Composition of the Gas Phase during the Reaction of Dimethyl Ether with Pyrogenic Evonik−Degussa AluC Dehydroxylated at 700 °C[a] and (b) Desorption of the Surface

(a) Composition of the Gas Phase during the Reaction of Dimethyl Ether with Pyrogenic Evonik−Degussa AluC Dehydroxylated at 700 °C		
Al_2O_3 with dimethyl ether	composition of the gas phase	
temperature	CH_3OCH_3	CH_4
room temperature	100%	0%
100 °C	100%	0%
200 °C	100%	0%
300 °C	42%	58%
(b) Desorption of the Surface (molecules/nm^2)		
hydrocarbon removed from the surface	molecules per nm^2	
ethylene	3.1×10^{-2}	
propylene	1.6×10^{-2}	
Z-2-butene	0.3×10^{-2}	
E-2-butene	0.7×10^{-2}	
isobutene	0.2×10^{-2}	
pentene	1.0×10^{-2}	

[a]Similar data are found for a boehmite-derived pure γ-Al_2O_3 provided by Sasol (SBA-200, see Table S1).

DOI: 10.1021/acscentsci.5b00226
ACS Cent. Sci. 2015, 1, 313−319

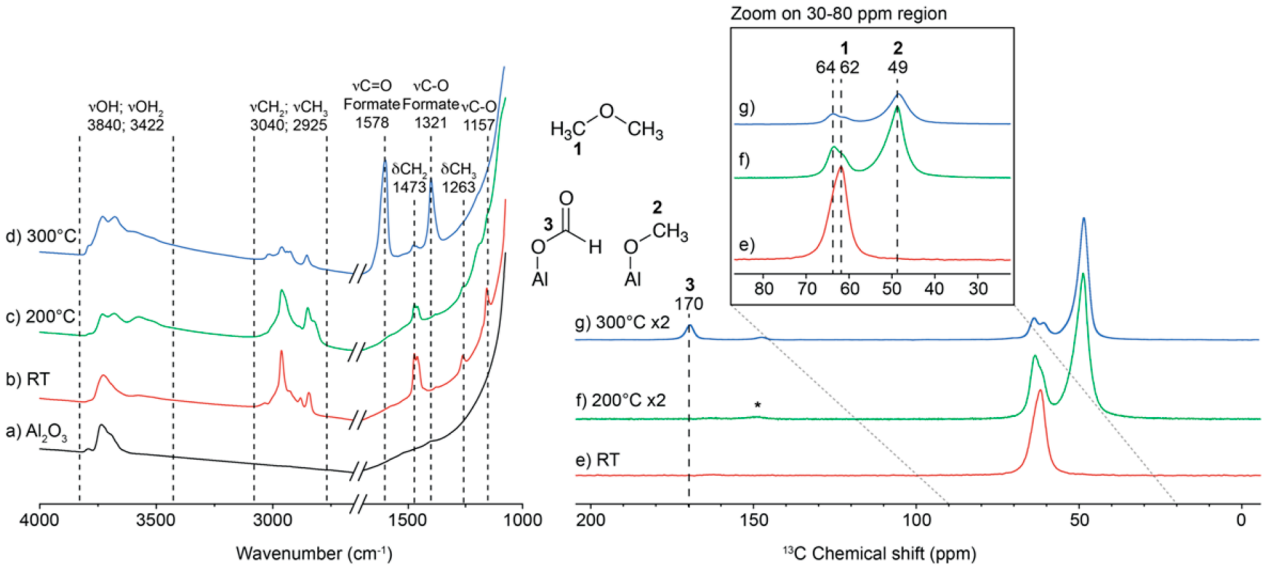

Figure 1. On the right: *in situ* FT-IR transmission spectra of (a) Al_2O_3 dehydroxylated at 700 °C, then reacted with dimethyl ether at room temperature (b), at 200 °C (c), and 300 °C (d) (for full spectra, see Figure S1). All the spectra were recorded with the gas phase condensed at −190 °C. In situ IR was used to determine the main changes of the surface species upon heating. We evidenced the activation of the C−O bond of DME as well as the formation of new surface species including formate. The same IR study can be found in Figure S2 for pure γ-Al_2O_3. On the left: $^1H-^{13}C$ CPMAS NMR, 400 MHz NMR spectrometer, spinning rate of 10 kHz. Spectrum of Al_2O_3 reacted with 2-^{13}C-$(CH_3)_2O$ (e) at room temperature, number of scans was set to 5k; (f) at 200 °C, number of scans was set to 100k; and (g) at 300 °C, number of scans was set to 50k. The recycling delay was set to 1 s of all the spectra. The radiofrequency field for ^1H excitation was set to 100 kHz.

to 2.7 CH_4 molecules per nm^2. This amount of methane approximately corresponds to one CH_4 per two Al sites considering the 110 surface of γ-Al_2O_3.[61,62] Treatment of the solids under high vacuum (10^{-5} mBar) at 100 °C led to desorption of ethene, propene, butenes, and pentenes as major products along with traces of hexenes according to GC and GC/MS (Table 1b). In contrast, no DME conversion was observed under the same reaction conditions in the absence of alumina, indicating that alumina is critical to promote the formation of these hydrocarbon products from DME.

To further understand the reaction, an *in situ* IR study was carried out. Figure 1a−d shows a series of IR spectra taken at different stages of the reaction (full IR spectrum are available in Figures S1 and S2, Supporting Information). Addition of DME to Al_2O_3 at room temperature (40 mbar, 4.6 molecules of DME per nm^2) led to the decrease of the intensity of the alumina OH bands at 3840 and 3600 cm^{-1} (Figure 1a,b).

It also showed the presence of CH_3 and CH_2 groups, a C−O bond as well as a few Csp_2-H species (tentatively attributed to the presence of a peak at 3040 cm^{-1}). At 200 °C two new peaks in the region of hydroxyl appeared (3570 and 3675 cm^{-1}), and the C−O band (1157 cm^{-1}) disappeared, consistent with the cleavage of that bond (Figure 1c). At 300 °C, the intensity of the ν(C−H) vibration decreased while the intensity of the OH band increased (Figure 1d). This was accompanied by the formation of methane in the gas phase and the appearance of two new peaks of strong intensity at 1578 and 1321 cm^{-1}, which can be assigned to the vibration of the C═O double bond and C−O bond of surface formate species.[63] Adsorbing methylformate on Al_2O_3 led to the appearance of the same bands, but also an additional band at 1683 associated with the carbonyl of physisorbed methyl formate (Figure S3). Similar bands were also obtained upon adsorption of formic acid on alumina.[64,65] Overall, these IR data suggest that carbon−carbon forming and carbon−oxygen cleavage reactions took place on the Al_2O_3 surfaces upon reaction with DME, while methane and formate species are formed.

The reaction was also monitored by solid-state NMR using ^{13}C dilabeled DME (Figure 1e−g). The insets e−g of Figure 1 show the ^{13}C cross polymerization magic angle spinning NMR (CP-MAS) spectra obtained on $Al_2O_{3-(700)}$ after reaction with DME at three different temperatures: 25, 200, and 300 °C. At low temperature, only one peak was observed at 62 ppm (Figure 1e), which is assigned to adsorbed DME. The intensity of the peak at 62 ppm decreased at higher temperatures, while a new peak progressively appeared at 49 ppm, reaching a maximum of intensity at 200 °C (Figure 1f). This peak is assigned to surface methoxy species.[58] In addition, a shoulder appeared at a higher field for the peak at 64 ppm that we assigned to the adsorption of DME molecule on different Al sites. Three peaks are observed in ^{13}C NMR after treatment at 300 °C (Figure 1g): Two at 49, 62−64 ppm assigned to methoxy and DME respectively, and a third one at 169 ppm assigned to formate. The observation of formate by carbon-13 NMR is also confirmed by 2D NMR: the carbon at 169 ppm, which is typical of an ester carbonyl, correlates with a proton at 9.2 ppm in the 2D NMR, which clearly identifies its attribution to a formate species (Figures S4−S6). In addition, adsorption of methyl formate on γ-$Al_2O_{3-(700)}$ leads to the same NMR signal consistent with its attribution to formate surface species (Figure S6) as previously discussed from the IR data. The correlation with the OCH_3 group suggests that the formate species are in close proximity to the methoxy species. No direct detection of hydrocarbons could be observed, suggesting that they are present in small amounts or remain adsorbed as minor alkoxy surface species.

The formation of methane, higher hydrocarbons, methoxy, and formate species was investigated by means of DFT periodic calculations. We used the 110 termination of γ-Al_2O_3 because it is the most abundant one for γ-Al_2O_3 (75%) and δ-Al_2O_3 (one of the component of our sample AluC) particles. In addition, this

DOI: 10.1021/acscentsci.5b00226
ACS Cent. Sci. 2015, 1, 313−319

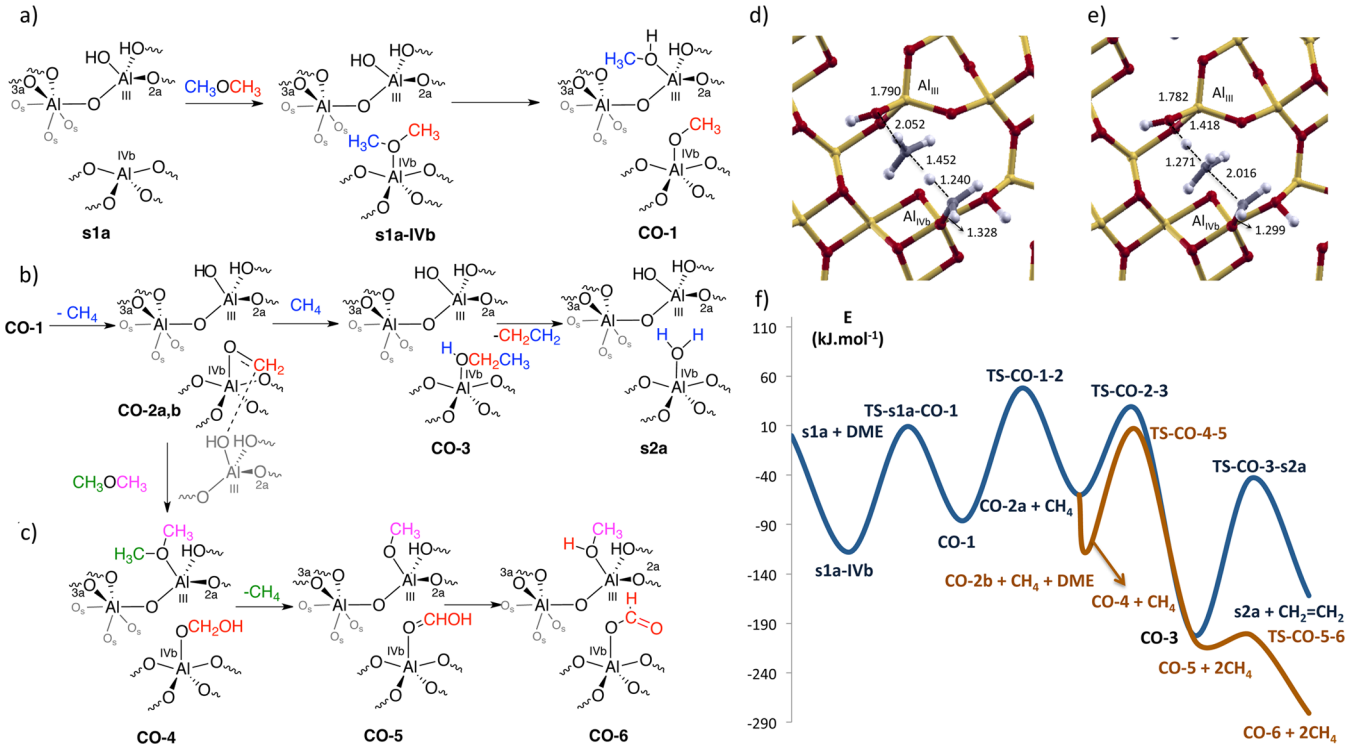

Figure 2. (a) C-OCH_3 activation process assisted by an OH group of the CH_3OCH_3 molecule on γ-Al_2O_3. (b) Formation of methane and oxonium, carbon−carbon bond formation step (from **CO-1** to **CO-3**) and subsequent ethylene formation along with s2a surface (c) Formate route from the CO-2 species. (d) Transition state structures corresponding to the formation of methane and oxonium (**TS-CO-1-2**) and (e) carbon−carbon bond formation steps (**TS-CO-2-3**). (f) Electronic energy profiles (in kJ mol^{-1}) for the ethylene and formate formation. The energies refer to two CH_3OCH_3 and the γ-Al_2O_3 surface. For the ethylene route (dark blue), the second DME molecule is not depicted since it does not participate in the reaction. The formate route is depicted in brown.

surface when completely dehydrated contains the most reactive sites (strong Lewis acid sites, see Figure S7).[61,62,66]

The adsorption (coordination) of CH_3OCH_3 on the most acidic Al_{III} site of the fully dehydrated alumina surface (**s0** surface, see Supporting Information) forms the species **0-III** in an exothermic step by 131 kJ mol^{-1}. This adsorbed species can further react through either the C−H or the C−O bonds of CH_3OCH_3. The C−O activation route with the transfer of the methoxy on the bare alumina surface is associated with a high-energy barrier equal to 179 kJ mol^{-1} and is endothermic by 16 kJ mol^{-1}.[67] On the more realistic monohydrated surfaces, the initial C−O activation step is lowered by more than 50 kJ mol^{-1} (vide infra). The alternative C−H bond activation pathway presents overall higher energy barriers and would also lead to the formation of unlikely Al-alkyl intermediates in the presence of proton sources (see Figure S8). In a previous study, we did an extensive analysis of the possible adsorption sites of water on the 110 termination of the γ-Al_2O_3 surface.[59] Depending on the initial adsorption site of water in the unit cell, corresponding to an OH coverage equal to 3.0 OH/nm^2, analogous energy profiles can be obtained for the ethylene formation route (see Supporting Information, Figure S9). Here, we will discuss ethylene formation from the most stable and probable **s1a** surface, in which one OH group coordinates to Al_{III} and one proton is bonded to the O_{2a} center, since the minima and the transition-states of the corresponding energy profile present the lowest energies of all the different surfaces evaluated with water initially adsorbed. From the **s1a** surface, the coordination of DME to the Al_{IVb} center yields a binding energy equal to 118 kJ mol^{-1} (**s1a-IVb** species in Figure 2a). In this case, the coordinated OH eases the CH_3 migration of the DME to produce the **CO-1** intermediate, via a barrier of 127 kJ mol^{-1} (hence significantly lower than for the nonwater asssisted process) and a reaction step endoenergetic by 31 kJ mol^{-1}. These results show that water assists the DME/methanol conversion as already proposed for acidic zeolites.[68,69] Hence, it is essential to generate Lewis acid sites adjacent to Lewis basic sites, so-called Frustrated Lewis acid base pairs, which display unexpected reactivities as more recently illustrated in molecular chemistry.[70] Overall, the participation of (frustrated) Lewis acid−base pairs, acidic Al_{III} and Al_{IVb} centers, and the basic oxygen atoms of both dimethyleter molecule and the OH group coordinated to such centers acts in a synergistic way providing a low energy pathway for the activation of DME.

After this step, the participation of two Al acid sites allows the previously transferred methyl group to abstract a hydride from the remaining methoxy group coordinated to Al_{IVb}, generating methane and a Al−O═CH_2 species with the O bound to AlIVb (**CO-2a** species in Figure 2b). In **CO2a** the −O═CH_2 species is not interacting with the OH group of AlIII while it is in **CO2b**.[71] In the corresponding transition-state (Figure 2d), a Al−O═CH_2^+ oxonium group is being formed along with methane. The oxonium species is characterized by a C═O distance equal to 1.328 Å at the transition-state, while the newly formed C−H bond has a distance equal to 1.452 Å and the one being broken equal to 1.240 Å (see Figure 2d). The formation of the oxonium has an energy barrier of 134 kJ mol^{-1} in a process endothermic by 26 kJ mol^{-1} when reaching **CO2a**. CH_4 can be released or subsequently undergo a C−H bond activation by the Al−O═CH_2^+ oxonium group leading to the formation of ethanol coordinated to Al_{IVb} (**CO-3** in Figure 2b).[58] This carbon−carbon

DOI: 10.1021/acscentsci.5b00226
ACS Cent. Sci. 2015, 1, 313−319

bond forming step is exoenergetic by 146 kJ mol^{-1} and has an energy barrier of 86 kJ mol^{-1}. The corresponding transition-state for the carbon−carbon bond formation step is shown as an inset in Figure 2e, in which the incoming carbon−carbon bond has a distance at the transition-state equal to 2.016 Å. Because of the structural similarity between **TS-CO-12** and **TS-CO-23** structures (corresponding to Figure 2d,e, respectively), there is also the possibility that from the **TS-CO-12** structure a slight rotation of the methane molecule could lead directly to the **TS-CO-23** structure. Finally, the formation of ethene (from the dehydration of the ethanol group in **CO-3** giving the hydrated termination **s2a** of the alumina surface in Figure 2b) has an energy barrier equal to 159 kJ mol^{-1} in a process endothermic by 40 kJ mol^{-1}. The formed water remains adsorbed on the Al_{IVb} center. Alcohol dehydration on γ-Al_2O_3 has been addressed previously both experimentally[44−47] and using DFT calculations on both 110 and 100 terminations.[44,48−52] While the 100 facet is more active than the 110 one toward alcohol dehydration,[50] both facets can allow this reaction, and the 110 facet exposes unsaturated Al_{III} and Al_{IVb} sites, which are significantly more reactive toward C−H activation and able to allow for the carbon−carbon bond formation from CH_3F to yield isobutene formation,[58] in contrast to the Al sites present in the 100 surface.[59] From the **CO-2** intermediate, in the event where the formed methane departs, an alternative route can lead to the formation of the formate species. The OH group present in Al_{III} can interact with the Al−O═CH_2^+ group in the Al_{IVb} via an interaction favorable by 57 kJ mol^{-1} (**CO-2b**). Subsequently, the OH group can decoordinate from the Al_{III} site, and a new DME molecule can coordinate to this Al center in a practically isoenergetic reaction (**CO-4** from Figure 2c). In a subsequent step a hydrogen is transferred from the CH_2 group of the Al_{IVb}−OCH_2−OH species to the DME molecule coordinated to Al_{III} in a process similar to that from **CO-1** to **CO-2a**. This step gives methane as product, while a O═CHOH group remains bonded to Al_{IVb} and a OCH_3 group to Al_{III} (**CO-5** species in Figure 2c). This step is exoenergetic (−95 kJ mol^{-1}) and associated with an energy barrier equal to 115 kJ mol^{-1}. Finally, the proton of the OH group can be transferred from the Al_{IVb}-OCHOH species to the Al_{III}-OCH_3 species via a very low energy barrier equal to 4 kJ mol^{-1} in a process exoergic by 76 kJ mol^{-1}.

The formation of formate and methanol adsorbed on the surface (**CO-6** species in Figure 2c) and two methane molecules is globally exoenergetic by 281 kJ mol^{-1} with respect to initial reactants (Al_2O_3 and two DME molecules), in agreement with the experimental observations. This route competes with ethylene formation in view of its similar energy barrier and more favorable thermodynamics. The whole energy profile for the formation of the ethylene from one DME molecule is shown in Figure 2f. In this energy profile, the energy barriers present values equal to 127−143 kJ mol^{-1}, except the elimination step which produces ethylene, which is slightly higher: 159 kJ mol^{-1}. All these barriers are accessible at 300 °C. From the partially hydrated alumina surface **s1a** and DME, the formation of ethylene and of the more hydrated alumina **s2a** surface is exothermic by 162 kJ mol^{-1}. From this **s2a** surface, the water adsorbed on the Al_{IVb} site can be exchanged by an incoming DME molecule regenerating the **s1a-IVb** species in an step endothermic by 44 kJ mol^{-1}. The formate route is very favored thermodynamically, being exothermic by more than 281 kJ mol^{-1} with respect to initial reactants, in agreement with the experimental observation of formate on the γ-Al_2O_3 surface. The formate route is kinetically favored without considering entropic contributions, since at the branching point in the energy profile the barrier is lower by 28 kJ mol^{-1}.

Overall, the formation of ethylene and water from DME is endoenergetic by 20 kJ mol^{-1}, while when including entropic contributions the reaction is exothermic by 85 kJ mol^{-1} (eq 1). By comparison, the formation of formate and methanol from DME and water is exothermic by 210 kJ mol (eq 2).

$$CH_3OCH_3 \rightarrow C_2H_4 + H_2O \quad \Delta G = -85\ \text{kJ}\cdot\text{mol}^{-1} \tag{1}$$

$$2CH_3OCH_3 + H_2O \rightarrow 2CH_4 + HCO_2H + CH_3OH \quad \Delta G = -210\ \text{kJ}\cdot\text{mol}^{-1} \tag{2}$$

In Gibbs free energy (see Supporting Information, Figure S10), the formate route is slightly more demanding than the ethylene route by 16 kJ mol^{-1}. The energy barriers for both ethylene and formate routes are higher due to the stabilization of the gas phase species. By including the entropic terms, the formation of ethylene and the **s2a** surface is exothermic by 146 kJ mol^{-1}, while the formate route leading to **CO-6** and two CH_4 molecules is exothermic by 209 kJ mol^{-1} (104 kJ mol^{-1} per DME molecule).

In conclusion, the reaction of DME on transition Al_2O_3 at 300 °C yields methane and higher olefins, which is reminiscent of the MTO process occurring on acidic zeolites. This reaction also generates methoxy and formate surface species according to IR and NMR data. These experiments and computational studies show that oxonium ions are key reaction intermediates. They form upon reaction of methoxy surface species with coordinated methanol on adjacent Al centers. The process involves C−H bond activation processes via a hydride abstraction from a surface methoxy species leading to a transition-state with methoxy, an oxonium group coordinated to Al_{III} and methane. The transient oxonium group can further react with methane yielding the first carbon−carbon bond or react with one additional DME molecule to form through a subsequent hydrogen transfer step a formate species, which was observed experimentally. These results show that the cooperation between adjacent aluminum sites of Al_2O_3 can readily participate in hydrogen transfer and C−C bond forming reaction processes. It also suggests that the "carbon pool" in the MTO process, which essentially takes place on the zeolite cavites of acidic zeolites via carbenium ions, can solely originate from methanol/DME and not from adventitious organic compounds. Higher hydrocarbons can be formed through the reaction of methanol/DME on highly acidic Al surface sites, which are also present in zeolites as part of the extraframework aluminum.

■ ASSOCIATED CONTENT

Supporting Information

The Supporting Information is available free of charge on the ACS Publications website at DOI: 10.1021/acscentsci.5b00226.

Details concerning preparation of the γ-Al_2O_3, additional NMR and IR spectra, and computational parameters (PDF)

■ AUTHOR INFORMATION

Corresponding Authors

*(C.C.) E-mail: ccoperet@ethz.ch.

*(P.S.) E-mail: Philippe.Sautet@ens-lyon.fr.

Author Contributions

#A.C.-V. and M.V. contributed equally.

DOI: 10.1021/acscentsci.5b00226
ACS Cent. Sci. 2015, 1, 313−319

Funding

Swiss National Foundation.

Notes

The authors declare no competing financial interest.

■ ACKNOWLEDGMENTS

A.C.-V. and M.V. acknowledge support from the Swiss National Foundation (Grant numbers PZ00P2_148059 and 200021_143600, respectively). We thank Evonik and Sassol for providing Alu C and Sba 200 alumina samples, respectively. Dr. D. Estes is acknowledged for helping with the edition of the manuscript.

■ REFERENCES

(1) Lunsford, J. H. Die Katalytische Oxidative Kupplung von Methan. *Angew. Chem.* **1995**, *107*, 1059−1070.
(2) Lunsford, J. H. The Catalytic Oxidative Coupling of Methane. *Angew. Chem., Int. Ed. Engl.* **1995**, *34*, 970−980.
(3) Crabtree, R. H. Aspects of Methane Chemistry. *Chem. Rev.* **1995**, *95*, 987−1007.
(4) Lunsford, J. H. Catalytic Conversion of Methane to More Useful Chemicals and Fuels: a Challenge for the 21st Century. *Catal. Today* **2000**, *63*, 165−174.
(5) Labinger, J. A.; Bercaw, J. E. Understanding and Exploiting C-H Bond Activation. *Nature* **2002**, *417*, 507−514.
(6) Woertink, J. S.; Smeets, P. J.; Groothaert, M. H.; Vance, M. A.; Sels, B. F.; Schoonheydt, R. A.; Solomon, E. I. A $[Cu_2O]^{2+}$ Core in Cu-ZSM-5, the Active Site in the Oxidation of Methane to Methanol. *Proc. Natl. Acad. Sci. U. S. A.* **2009**, *106*, 18908−18913.
(7) Crabtree, R. H. Introduction to Selective Functionalization of C-H Bonds. *Chem. Rev.* **2010**, *110*, 575−575.
(8) Copéret, C. C-H Bond Activation and Organometallic Intermediates on Isolated Metal Centers on Oxide Surfaces. *Chem. Rev.* **2010**, *110*, 656−680.
(9) Schwarz, H. Chemie mit Methan: Studieren geht über Probieren! *Angew. Chem.* **2011**, *123*, 10276−10297.
(10) Schwarz, H. Chemistry with Methane: Concepts Rather than Recipes. *Angew. Chem., Int. Ed.* **2011**, *50*, 10096−10115.
(11) Hazari, N.; Iglesia, E.; Labinger, J. A.; Simonetti, D. A. Selective Homogeneous and Heterogeneous Catalytic Conversion of Methanol/Dimethyl Ether to Triptane. *Acc. Chem. Res.* **2012**, *45*, 653−662.
(12) Schwarz, H. How and Why Do Cluster Size, Charge State, and Ligands Affect the Course of Metal-Mediated Gas-Phase Activation of Methane? *Isr. J. Chem.* **2014**, *54*, 1413−1431.
(13) Kwapien, K.; Paier, J.; Sauer, J.; Geske, M.; Zavyalova, U.; Horn, R.; Schwach, P.; Trunschke, A.; Schlögl, R. Zentren der Methanaktivierung auf Oberflächen von Lithium-dotiertem MgO. *Angew. Chem.* **2014**, *126*, 8919−8923.
(14) Kwapien, K.; Paier, J.; Sauer, J.; Geske, M.; Zavyalova, U.; Horn, R.; Schwach, P.; Trunschke, A.; Schlögl, R. Sites for Methane Activation on Lithium-Doped Magnesium Oxide Surfaces. *Angew. Chem., Int. Ed.* **2014**, *53*, 8774−8778.
(15) Tsai, M.-L.; Hadt, R. G.; Vanelderen, P.; Sels, B. F.; Schoonheydt, R. A.; Solomon, E. I. $[Cu_2O]^{2+}$ Active Site Formation in Cu-ZSM-5: Geometric and Electronic Structure Requirements for N_2O Activation. *J. Am. Chem. Soc.* **2014**, *136*, 3522−3529.
(16) Tian, P.; Wei, Y.; Ye, M.; Liu, Z. Methanol to Olefins (MTO): From Fundamentals to Commercialization. *ACS Catal.* **2015**, *5*, 1922−1938.
(17) Stöcker, M. Methanol to Olefins (MTO) and Methanol to Gasoline (MTG). In *Zeolites and Catalysis*; Cejka, J., Corma, A., Zones, S., Eds.; Wiley-VCH Verlag GmbH & Co. KGaA: Weinheim, 2010; pp 687−711.
(18) Haw, J. F.; Song, W.; Marcus, D. M.; Nicholas, J. B. The Mechanism of Methanol to Hydrocarbon Catalysis. *Acc. Chem. Res.* **2003**, *36*, 317−326.
(19) Marcus, D. M.; McLachlan, K. A.; Wildman, M. A.; Ehresmann, J. O.; Kletnieks, P. W.; Haw, J. F. Experimental Evidence from H/D Exchange Studies for the Failure of Direct C-C Coupling Mechanisms in the Methanol-to-Olefin Process Catalyzed by HSAPO-34. *Angew. Chem., Int. Ed.* **2006**, *45*, 3133−3136.
(20) McCann, D. M.; Lesthaeghe, D.; Kletnieks, P. W.; Guenther, D. R.; Hayman, M. J.; Van Speybroeck, V.; Waroquier, M.; Haw, J. F. A Complete Catalytic Cycle for Supramolecular Methanol-to-Olefins Conversion by Linking Theory with Experiment. *Angew. Chem., Int. Ed.* **2008**, *47*, 5179−5182.
(21) Van Speybroeck, V.; De Wispelaere, K.; Van der Mynsbrugge, J.; Vandichel, M.; Hemelsoet, K.; Waroquier, M. First principle chemical kinetics in zeolites: the methanol-to-olefin process as a case study. *Chem. Soc. Rev.* **2014**, *43*, 7326−7357.
(22) Blaszkowski, S. R.; van Santen, R. A. Theoretical Study of C-C Bond Formation in the Methanol-to-Gasoline Process. *J. Am. Chem. Soc.* **1997**, *119*, 5020−5027.
(23) Tajima, N.; Tsuneda, T.; Toyama, F.; Hirao, K. A New Mechanism for the First Carbon-Carbon Bond Formation in the MTG Process: A Theoretical Study. *J. Am. Chem. Soc.* **1998**, *120*, 8222−8229.
(24) Li, J.; Wei, Z.; Chen, Y.; Jing, B.; He, Y.; Dong, M.; Jiao, H.; Li, X.; Qin, Z.; Wang, J.; Fan, W. A route to form initial hydrocarbon pool species in methanol conversion to olefins over zeolites. *J. Catal.* **2014**, *317*, 277−283.
(25) Lesthaeghe, D.; Van Speybroeck, V.; Marin, G. B.; Waroquier, M. Understanding the failure of direct C-C coupling in the zeolite-catalyzed methanol-to-olefin process. *Angew. Chem., Int. Ed.* **2006**, *45*, 1714−1719.
(26) Sun, X.; Mueller, S.; Liu, Y.; Shi, H.; Haller, G. L.; Sanchez-Sanchez, M.; van Veen, A. C.; Lercher, J. A. On reaction pathways in the conversion of methanol to hydrocarbons on HZSM-5. *J. Catal.* **2014**, *317*, 185−197.
(27) Olah, G. A.; Doggweiler, H.; Felberg, J. D.; Frohlich, S.; Grdina, M. J.; Karpeles, R.; Keumi, T.; Inaba, S.-i.; Ip, W. M.; Lammertsma, K.; Salem, G.; Tabor, D. Onium Ylide chemistry. 1. Bifunctional acid-base-catalyzed conversion of heterosubstituted methanes into ethylene and derived hydrocarbons. The onium ylide mechanism of the C1 -> C2 conversion. *J. Am. Chem. Soc.* **1984**, *106*, 2143−2149.
(28) Stöcker, M. Methanol-to-hydrocarbons: catalytic materials and their behavior. *Microporous Mesoporous Mater.* **1999**, *29*, 3−48.
(29) Hemelsoet, K.; Van der Mynsbrugge, J.; De Wispelaere, K.; Waroquier, M.; Van Speybroeck, V. Unraveling the Reaction Mechanisms Governing Methanol-to-Olefins Catalysis by Theory and Experiment. *ChemPhysChem* **2013**, *14*, 1526−1545.
(30) Olsbye, U.; Svelle, S.; Bjørgen, M.; Beato, P.; Janssens, T. V. W.; Joensen, F.; Bordiga, S.; Lillerud, K. P. Umwandlung von Methanol in Kohlenwasserstoffe: Wie Zeolith-Hohlräume und Porengröße die Produktselektivität bestimmen. *Angew. Chem.* **2012**, *124*, 5910−5933.
(31) Olsbye, U.; Svelle, S.; Bjørgen, M.; Beato, P.; Janssens, T. V. W.; Joensen, F.; Bordiga, S.; Lillerud, K. P. Conversion of Methanol to Hydrocarbons: How Zeolite Cavity and Pore Size Controls Product Selectivity. *Angew. Chem., Int. Ed.* **2012**, *51*, 5810−5831.
(32) Dahl, I. M.; Kolboe, S. On the Reaction-Mechanism for Propene Formation in the Mto Reaction over Sapo-34. *Catal. Lett.* **1993**, *20*, 329−336.
(33) Dahl, I. M.; Kolboe, S. On the Reaction-Mechanism for Hydrocarbon Formation from Methanol over Sapo-34 0.1. Isotopic Labeling Studies of the Co-Reaction of Ethene and Methanol. *J. Catal.* **1994**, *149*, 458−464.
(34) Dahl, I. M.; Kolboe, S. On the reaction mechanism for hydrocarbon formation from methanol over SAPO-34 0.2. Isotopic labeling studies of the co-reaction of propene and methanol. *J. Catal.* **1996**, *161*, 304−309.
(35) Lesthaeghe, D.; Van der Mynsbrugge, J.; Vandichel, M.; Waroquier, M.; Van Speybroeck, V. Full Theoretical Cycle for both Ethene and Propene Formation during Methanol-to-Olefin Conversion in H-ZSM-5. *ChemCatChem* **2011**, *3*, 208−212.

DOI: 10.1021/acscentsci.5b00226
ACS Cent. Sci. 2015, 1, 313−319

(36) Lesthaeghe, D.; Van Speybroeck, V.; Marin, G. B.; Waroquier, M. What Role do Oxonium Ions and Oxonium Ylides play in the ZSM-5 Catalysed Methanol-to-Olefin Process? *Chem. Phys. Lett.* **2006**, *417*, 309−315.
(37) Silaghi, M.-C.; Chizallet, C.; Raybaud, P. Challenges on molecular aspects of dealumination and desilication of zeolites. *Microporous Mesoporous Mater.* **2014**, *191*, 82−96.
(38) Corma, A.; Martinez, A.; Martinez, C. The role of extraframework aluminum species in USY catalysts during isobutane/2-butene alkylation. *Appl. Catal., A* **1996**, *134*, 169−182.
(39) Cejka, J., Corma, A.; Zones, S. *Zeolites and Catalysis: Synthesis, Reactions and Applications*; Wiley-VCH: Weinheim, 2010.
(40) Chang, C. D. Hydrocarbons from Methanol. *Catal. Rev.: Sci. Eng.* **1983**, *25*, 1−118.
(41) Xu, M.; Lunsford, J. H.; Goodman, D. W.; Bhattacharyya, A. Synthesis of dimethyl ether (DME) from methanol over solid-acid catalysts. *Appl. Catal., A* **1997**, *149*, 289−301.
(42) Yaripour, F.; Baghaei, F.; Schmidt, I.; Perregaard, J. Catalytic dehydration of methanol to dimethyl ether (DME) over solid-acid catalysts. *Catal. Commun.* **2005**, *6*, 147−152.
(43) Schiffino, R. S.; Merrill, R. P. A mechanistic study of the methanol dehydration reaction on.gamma.-alumina catalyst. *J. Phys. Chem.* **1993**, *97*, 6425−6435.
(44) Roy, S.; Mpourmpakis, G.; Hong, D.-Y.; Vlachos, D. G.; Bhan, A.; Gorte, R. J. Mechanistic Study of Alcohol Dehydration on γ-Al_2O_3. *ACS Catal.* **2012**, *2*, 1846−1853.
(45) Kang, M.; DeWilde, J. F.; Bhan, A. Kinetics and Mechanism of Alcohol Dehydration on γ-Al_2O_3: Effects of Carbon Chain Length and Substitution. *ACS Catal.* **2015**, *5*, 602−612.
(46) DeWilde, J. F.; Chiang, H.; Hickman, D. A.; Ho, C. R.; Bhan, A. Kinetics and Mechanism of Ethanol Dehydration on γ-Al_2O_3: The Critical Role of Dimer Inhibition. *ACS Catal.* **2013**, *3*, 798−807.
(47) Phung, T. K.; Lagazzo, A.; Rivero Crespo, M. Á.; Sánchez Escribano, V.; Busca, G. A study of commercial transition aluminas and of their catalytic activity in the dehydration of ethanol. *J. Catal.* **2014**, *311*, 102−113.
(48) Christiansen, M. A.; Mpourmpakis, G.; Vlachos, D. G. Density Functional Theory-Computed Mechanisms of Ethylene and Diethyl Ether Formation from Ethanol on γ-Al_2O_3(100). *ACS Catal.* **2013**, *3*, 1965−1975.
(49) Jenness, G. R.; Christiansen, M. A.; Caratzoulas, S.; Vlachos, D. G.; Gorte, R. J. Site-Dependent Lewis Acidity of γ-Al_2O_3 and Its Impact on Ethanol Dehydration and Etherification. *J. Phys. Chem. C* **2014**, *118*, 12899−12907.
(50) Kwak, J. H.; Rousseau, R.; Mei, D.; Peden, C. H. F.; Szanyi, J. The Origin of Regioselectivity in 2-Butanol Dehydration on Solid Acid Catalysts. *ChemCatChem* **2011**, *3*, 1557−1561.
(51) Christiansen, M. A.; Mpourmpakis, G.; Vlachos, D. G. DFT-driven multi-site microkinetic modeling of ethanol conversion to ethylene and diethyl ether on γ-Al_2O_3 (111). *J. Catal.* **2015**, *323*, 121−131.
(52) Larmier, K.; Chizallet, C.; Cadran, N.; Maury, S.; Abboud, J.; Lamic-Humblot, A.-F.; Marceau, E.; Lauron-Pernot, H. Mechanistic investigation of isopropanol conversion on alumina catalysts: location of active sites for alkene/ether production. *ACS Catal.* **2015**, *5*, 4423−4437.
(53) Chen, J. G.; Basu, P.; Ballinger, T. H.; Yates, J. T. A transmission infrared spectroscopic investigation of the reaction of dimethyl ether with alumina surfaces. *Langmuir* **1989**, *5*, 352−356.
(54) Kipnis, M. A.; Samokhin, P. V.; Volnina, E. A.; Lin, G. I. Surface reactions of dimethyl ether on γ-Al_2O_3: 1. Adsorption and thermal effects. *Kinet. Catal.* **2014**, *55*, 456−462.
(55) Wischert, R.; Copéret, C.; Delbecq, F.; Sautet, P. Dinitrogen: a selective probe for tri-coordinate Al ″defect″ sites on alumina. *Chem. Commun.* **2011**, *47*, 4890−4892.
(56) Wischert, R.; Copéret, C.; Delbecq, F.; Sautet, P. Optimal Water Coverage on Alumina: A Key to Generate Lewis Acid−Base Pairs that are Reactive Towards the C-H Bond Activation of Methane. *Angew. Chem.* **2011**, *123*, 3260−3263.
(57) Wischert, R.; Copéret, C.; Delbecq, F.; Sautet, P. Optimal Water Coverage on Alumina: A Key to Generate Lewis Acid−Base Pairs that are Reactive Towards the C-H Bond Activation of Methane. *Angew. Chem., Int. Ed.* **2011**, *50*, 3202−3205.
(58) Comas-Vives, A.; Schwarzwälder, M.; Copéret, C.; Sautet, P. Carbon−Carbon Bond Formation by Activation of CH_3F on Alumina. *J. Phys. Chem. C* **2015**, *119*, 7156−7163.
(59) Wischert, R.; Laurent, P.; Copéret, C.; Delbecq, F.; Sautet, P. γ-Alumina: The Essential and Unexpected Role of Water for the Structure, Stability, and Reactivity of ″Defect″ Sites. *J. Am. Chem. Soc.* **2012**, *134*, 14430−14449.
(60) Note that above 300 °C the dimethyl ether undergoes a homolytic cleavage of the CH_3−OCH_3 bond leaving two radicals in the gas phase which can react with the alumina surface. For this reason, the system will not be studied above 300 °C (see ref 27).
(61) Digne, M.; Sautet, P.; Raybaud, P.; Euzen, P.; Toulhoat, H. Hydroxyl Groups on γ-Alumina Surfaces: A DFT Study. *J. Catal.* **2002**, *211*, 1−5.
(62) Digne, M.; Sautet, P.; Raybaud, P.; Euzen, P.; Toulhoat, H. Use of DFT to Achieve a Rational Understanding of Acid-Basic Properties of γ-Alumina Surfaces. *J. Catal.* **2004**, *226*, 54−68.
(63) Rataboul, F.; Baudouin, A.; Thieuleux, C.; Veyre, L.; Copéret, C.; Thivolle-Cazat, J.; Basset, J.-M.; Lesage, A.; Emsley, L. Molecular Understanding of the Formation of Surface Zirconium Hydrides upon Thermal Treatment under Hydrogen of $[(\equiv SiO)Zr(CH_2tBu)_3]$ by Using Advanced Solid-State NMR Techniques. *J. Am. Chem. Soc.* **2004**, *126*, 12541−12550.
(64) Koga, O.; Onishi, T.; Tamaru, K. Infrared emission spectra of formic acid adsorbed on alumina. *J. Chem. Soc., Chem. Commun.* **1974**, 464−464.
(65) Rubasinghege, G.; Ogden, S.; Baltrusaitis, J.; Grassian, V. H. Heterogeneous Uptake and Adsorption of Gas-Phase Formic Acid on Oxide and Clay Particle Surfaces: The Roles of Surface Hydroxyl Groups and Adsorbed Water in Formic Acid Adsorption and the Impact of Formic Acid Adsorption on Water Uptake. *J. Phys. Chem. A* **2013**, *117*, 11316−11327.
(66) Krokidis, X.; Raybaud, P.; Gobichon, A. E.; Rebours, B.; Euzen, P.; Toulhoat, H. Theoretical Study of the Dehydration Process of Boehmite to γ-alumina. *J. Phys. Chem. B* **2001**, *105*, 5121−5130.
(67) An energy barrier of 100 kJ·mol^{-1} at 25 °C is equivalent in rate to an energy barrier equal to 195 kJ·mol^{-1} at 300 °C.
(68) Jones, A. J.; Iglesia, E. Kinetic, Spectroscopic, and Theoretical Assessment of Associative and Dissociative Methanol Dehydration Routes in Zeolites. *Angew. Chem., Int. Ed.* **2014**, *53*, 12177−12181.
(69) Blaszkowski, S. R.; van Santen, R. A. Theoretical Study of the Mechanism of Surface Methoxy and Dimethyl Ether Formation from Methanol Catalyzed by Zeolitic Protons. *J. Phys. Chem. B* **1997**, *101*, 2292−2305.
(70) Stephan, D. W.; Erker, G. Frustrated Lewis Pairs: Metal-free Hydrogen Activation and More. *Angew. Chem., Int. Ed.* **2010**, *49*, 46−76.
(71) In ref 58, we proposed the analogous pathway for the formation of an ethoxy intermediate taking CH_3F as initial substrate.

DOI: 10.1021/acscentsci.5b00226
ACS Cent. Sci. 2015, 1, 313−319